Location of Single-Particle Levels in Medium Mass Nuclei*

B. L. COHEN, R. H. FULMER, AND A. L. MCCARTHY
University of Pittsburgh, Pittsburgh, Pennsylvania

(Received November 10, 1961)

The levels of Ni^{59}, Ni^{61}, Fe^{57}, and Ti^{49} are studied with (d,p) reactions; angular distributions and absolute cross sections are analyzed with the aid of distorted-wave Born approximation calculations. Essentially all levels in the Ni isotopes up to about 1-Mev binding energy are assigned to a shell-model state and their reduced widths are measured. From this, the "center of gravity" of each shell-model state is determined. The results are very much different from those of Schiffer, Lee, and Zeidman, and much closer to theoretical expectations. For example, there is a large energy gap between major shells, the energy of the $3s_{1/2}$ state agrees with other evidence, the semiclosed-shell behavior of 40 and 56 neutrons is explained, etc. The widths of the energy distributions of levels belonging to single shell-model states agree well with the predictions of the giant resonance theory of Lane, Thomas, and Wigner.

I. INTRODUCTION

A VERY interesting study of the neutron single-particle states in the nickel region has been reported by Schiffer, Lee, and Zeidman.[1] In their measurements of the energy spectra of protons from (d,p) reactions with poor energy resolution, they found a series of peaks which they interpreted as due to single-particle levels in the giant resonance sense.[2] They assigned these to definite shell-model states by application of Butler stripping theory[3] to the measured angular distributions. These assignments were further supported by the measured relative reduced widths, again interpreted by use of Butler theory. Their results contained many surprising aspects, for example:

(1) The $3s_{1/2}$ state falls at a binding energy of about 3 Mev, whereas the neutron giant resonance,[4] due to this same $3s_{1/2}$ state, is at zero binding energy in this mass region.

(2) The difference in binding energy of the $3s_{1/2}$ state between masses 60 and 90–120 is too small to be explained by the usual theory.[5]

(3) There is somewhat more change in the relative energies of the various levels between nuclei of approximately the same mass than one would expect.

(4) The energy gap between the major shells is no larger than a typical energy gap between subshells; if this were actually the case, there would be no closed shell effects in nuclei. It might be argued that the energy gap between the major shells widens as the mass increases, so that it is much wider when the levels bordering it begin to fill. However, there is no evidence for significant changes in this gap with mass in existing calculations.[6]

In view of these surprising results, it seems desirable to make a more detailed experimental study of the problem. In this paper we report such a study in Ni^{58}, Ni^{60}, Fe, and Ti, carried out with an order of magnitude better resolution than that used in reference 1; this enables us to study each individual nuclear level and to make the transition to the gross structure problem by computation. This method is much more laborious, but of course it is much more trustworthy than the method of reference 1. In addition, our data analysis was carried out using distorted-wave Born approximation (DWBA) calculations[7] rather than Butler theory. This gives much better and more detailed fits to the angular distributions, and the absolute reduced widths determined by this method are far more reliable and useful than the relative reduced widths derived from Butler theory.

The (d,p) reactions on Ni^{58} and Ni^{60} have previously been studied with high resolution ($\sim$8 kev) by Paris,[8] and by Enge and Fisher,[9] using 7.5-Mev deuterons. They accurately determined the energies of the levels in the final nuclei, and assigned values for l, the angular momentum with which the neutron enters the nucleus, for many levels in Ni^{61}. Dalton *et al.*[10] made a similar study with 8.9-Mev deuterons and 70-kev resolution.

The principal advantage of the present work over these is that the higher bombarding energy and DWBA calculations allow the study to be extended to higher

* Supported by the National Science Foundation and the Office of Naval Research.

[1] J. P. Schiffer, L. L. Lee, Jr., and B. Zeidman, Phys. Rev. **115**, 427 (1959).

[2] A. M. Lane, R. G. Thomas, and E. P. Wigner, Phys. Rev. **98**, 693 (1955).

[3] S. T. Butler, Proc. Roy. Soc. (London) **A208**, 559 (1951).

[4] H. Feshbach, C. E. Porter, and V. F. Weisskopf, Phys. Rev. **96**, 448 (1954).

[5] B. L. Cohen and R. E. Price, Nuclear Phys. **17**, 129 (1960).

[6] A. Shroder, Nuovo cimento **7**, 461 (1958). A. A. Ross, H. Mark, and R. D. Lawson, Phys. Rev. **102**, 1613 (1956); **104**, 401 (1956).

[7] G. R. Satchler, R. Bassel, R. Drisko, and E. Rost (private communications). The authors are greatly indebted to Dr. Satchler and his group for performing these DWBA calculations for the cases of interest here. They are based on the theory of Tobocman [Phys. Rev. **94**, 1655 (1954); Phys. Rev. **115**, 99 (1959)]. The optical potentials used are of the Saxon form; for the deuterons $V=55$ Mev, $W=20$ Mev, $R=1.5A^{\frac{1}{3}}$ f, $a=0.6$ f, while for the protons $V=(58-\frac{1}{2}E_p)$ Mev, $W=(4+\frac{1}{4}E_p)$ Mev, $R=1.3A^{\frac{1}{3}}$ f, $a=0.5$ f. The matching radius for the captured neutron wave function is $R_N=6.3$ f. See also R. M. Drisko, R. H. Bassel, G. R. Satchler, Oak Ridge National Laboratory Report ORNL-3085 (unpublished).

[8] C. H. Paris, Massachusetts Institute of Technology Laboratory for Nuclear Science Progress Report, May 1, 1959 (unpublished), p. 116.

[9] H. A. Enge and R. A. Fisher, Massachusetts Institute of Technology Laboratory for Nuclear Science Progress Report, May 1, 1959 (unpublished), p. 124.

[10] A. W. Dalton, G. Parry, H. D. Scott, and S. Swierszczewski, Proc. Phys. Soc. **77**, 682 (1961).

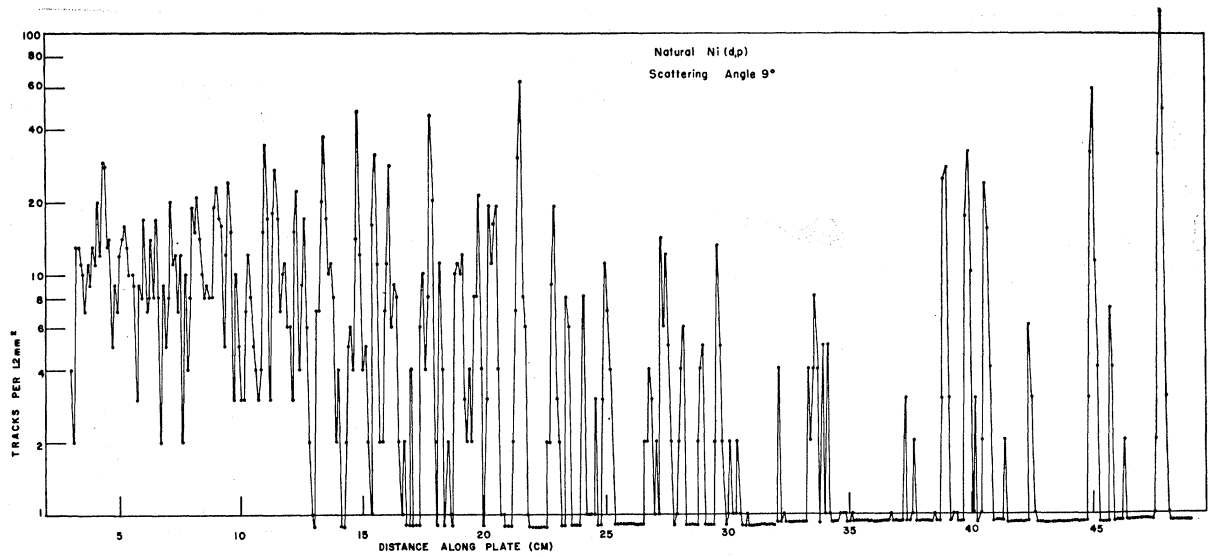

FIG. 1. Measured proton energy spectrum from (d,p) reactions on the natural nickel target. Points below one denote zero counts in the area scanned. The peaks due to Ni^{58} may be identified from Fig. 2. Energy resolution here is about 25 kev; it is better than in any other part of this experiment.

excitation energies and more identifications to be made. The analysis is carried much further than in references 8, 9, and 10; the "centers of gravity" of the single-particle levels are determined and their widths are estimated; these are then compared with the results of reference 1 and with theory.

II. EXPERIMENTAL PROCEDURE

The basic experimental method has been described previously[11] and is applied here with two major improvements. First, an accurate energy calibration of the magnetic spectrograph has been made using the proton groups from O, C, F, and Mg(d,p) reactions whose energies are well known. Secondly, better energy resolution was obtained in much of the data by using thinner targets and paying more attention to details. A natural Ni target in the form of a narrow strip of thickness 0.62 mg/cm² was used to produce spectra with 25-kev resolution at four scattering angles; an example of these data is shown in Fig. 1. These spectra resolve closely spaced levels and provide an accurate determination of peak energies, but are less accurate

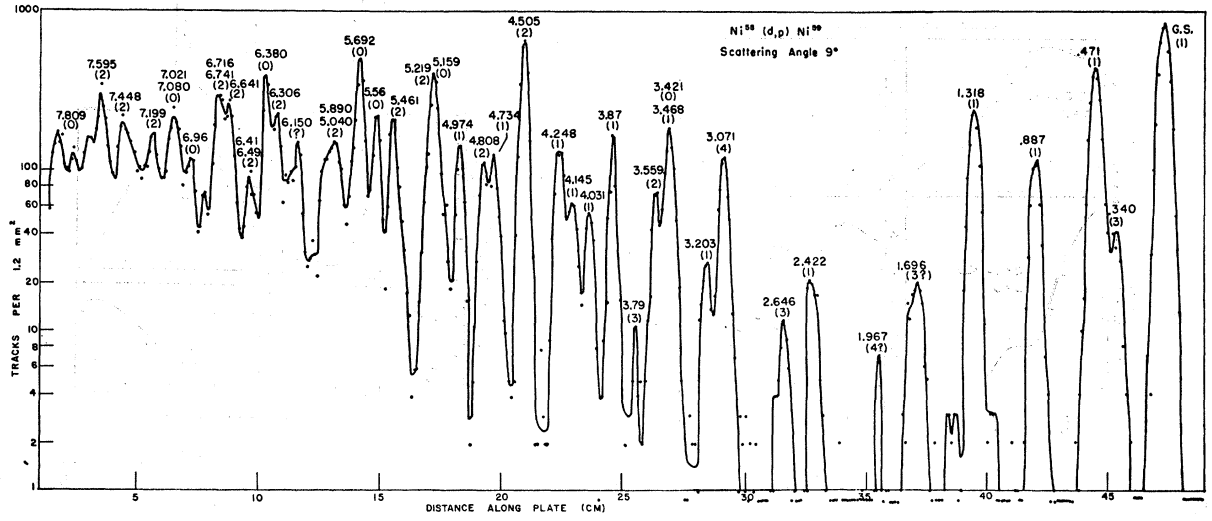

FIG. 2. Measured proton energy spectrum from $Ni^{58}(d,p)$. Numbers above peaks are excitation energies in Ni^{59} in Mev; l values assigned to these peaks are in parentheses. Angle of observation is 9°.

[11] B. L. Cohen, J. B. Mead, R. E. Price, K. Quisenberry, and C. Martz, Phys. Rev. **118**, 499 (1960).

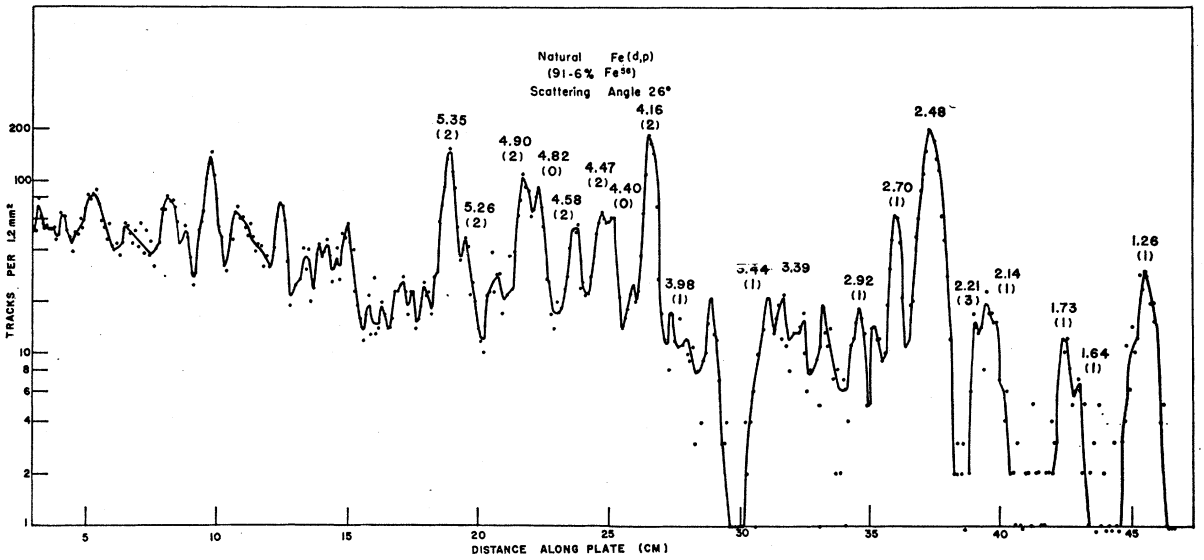

FIG. 3. Measured proton energy spectrum from Fe(d,p). Numbers above peaks are excitation energies in Fe^{57} in Mev, and l values assigned to these peaks are in parentheses. Angle of observation is 26°. Energy resolution here is considerably poorer than in any other part of the experiment.

for cross section determinations. Target thicknesses for Fe, Ti, Ni^{60}, and Ni^{58} were, respectively, 3.2, 1.5, 2.0, and 2.2 mg/cm². Typical spectra for some of these are shown in Figs. 2 and 3.

Data from Fe(d,p) reactions below $Q=4.4$ Mev were taken at 13 scattering angles. The angular distributions of some of the proton groups are compared with the DWBA calculations[7] in Fig. 4. Of the 19 peaks which have been analyzed, nine have distributions comparable to those of Fig. 4(a–d). Most of these peaks are well separated from those of the next-nearest energy levels known from reference 12. Eight of the peaks give less satisfactory angular distributions which, however, can still be used to assign l values. Of these, six have distributions comparable to the DWBA curves to about 30° but have higher intensities at larger angles. Two of the nineteen peaks have angular distributions which cannot be explained by the theory [see Fig. 4(e)].

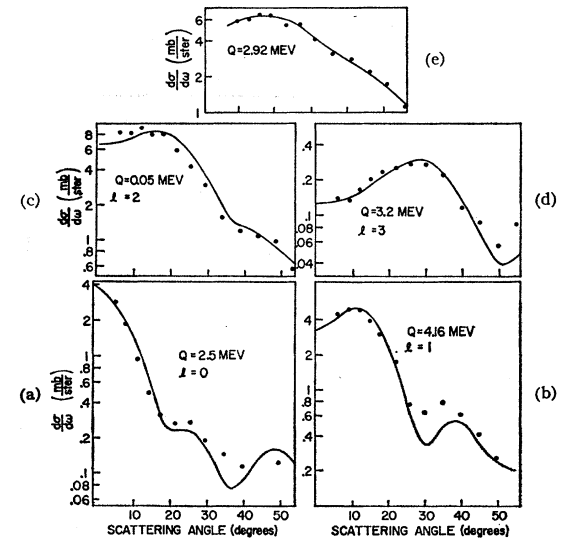

FIG. 4. Measured angular distributions for certain peaks from Fe(d,p) reactions and comparison with DWBA calculations. (a)–(d) are typical examples of angular distributions fitted by $l=0$, 1, 2, and 3, respectively. In these figures the solid line is the DWBA curve. (e) shows an angular distribution which is not fitted by calculated angular distributions for any single l value. The solid line is an experimental curve.

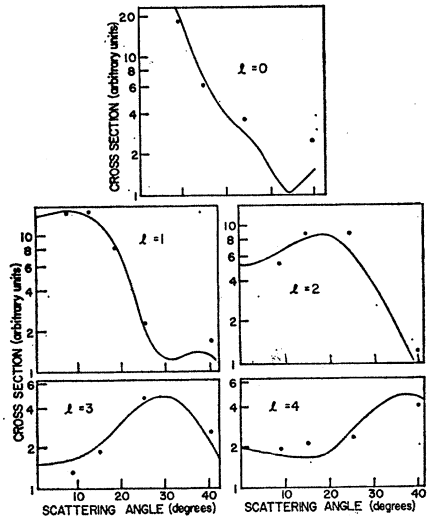

FIG. 5. Illustrations of assignment of l values by the four angle method described in text. The four points are experimental, and the curves show the DWBA calculations.

[12] A. Sperduto, Massachusetts Institute of Technology Laboratory for Nuclear Science Annual Progress Report, June, 1957–May, 1958 (unpublished), p. 130.

TABLE I. $Ni^{60}(d,p)Ni^{61}$.

This paper					MIT reports				Dalton *et al.*			Scott
(1)	(2)	(3)	(4)	(5)	(6)	(7)	(8)	(9)	(10)	(11)	(12)	(13)
Excitation energy (Mev)	l	J	$\left(\frac{d\sigma}{d\omega}\right)_{max}$ (mb/sr)	$(2J_f+1)S$	Excitation energy (Mev)	l_n	$\left(\frac{d\sigma}{d\omega}\right)_{max}$ (mb/sr)	$\frac{d\sigma}{d\omega}(30°)$ (relative)	Excitation energy (Mev)	l_n	$\left(\frac{d\sigma}{d\omega}\right)_{max}$ (mb/sr)	$(2J_f+1)S$
0	1	3/2	9.50	1.58	0	1	1.528	1	0	1	6.0	1.11
0.069	3	5/2	1.91	3.52	0.068	3	0.246	0.249	···	3	1.98	2.87
0.290	1	1/2	7.13	1.15	0.284	1	1.154	0.770	0.28	1	4.34	0.82
0.654	1	1/2	0.173	0.026	0.660	···		0.022(50°)	0.67	1	0.204	
0.908	3	5/2	0.145	0.241	0.915	···		0.046				
1.105	1	1/2	0.880	0.125	1.104	1	0.131	0.138				
1.139					1.137	···	···	0.036	1.20	1	1.86	0.31
1.195	1	1/2	1.55	0.218	1.190	1	0.311	0.264				
1.454	3	5/2	0.143	0.223	1.460	···		0.056				
1.750	1	1/2	0.228	0.028	1.735	1	0.067	0.035				
2.133	4	9/2	1.98	6.2	2.127	1	0.615	0.641	2.17		1.82	
2.133	1	1/2	2.20	0.265								
					2.599	1	0.112	0.007				
					2.645	···	···	0.108				
2.694	2	5/2	3.05	0.725	2.704	2	0.387	0.570	2.75	2	2.20	
2.780	1	1/2	0.735	0.078	2.770	1	0.090	0.099				
2.905	0	1/2	0.180	0.009	2.907	···	···	0.023				
3.086	0	1/2	1.54	0.077	3.069	0	0.980	0.319	3.10	0	3.15	0.052
3.305	3	5/2	0.253	0.281	3.294	···	···	0.097				
3.494	2	5/2	5.00	1.04	3.503	2	0.998	1.287	3.54	2	3.91	
3.649	2	5/2	1.13	0.236	3.643	···		0.313				
3.743	0	1/2	3.48	0.158	3.749	···		0.587	3.77	0	6.59	
3.877	2	5/2	0.78	0.153	3.875	···		0.123				
3.923	3	5/2	0.602	0.628	3.938	···		0.055				
4.07	3	5/2	0.133	0.137	4.078	···		0.012				
4.146	2	5/2	0.390	0.074	4.158			0.169				
4.234	1	1/2	0.712	0.063	4.247	1, 2	0.096	0.166				
4.386	2	5/2	1.32	0.245	4.369	···		0.215				
					4.381	···		0.210				
4.472	2	5/2	1.34	0.244	4.471	···		0.412	4.49			
4.760	2	5/2	4.71	0.79	4.756	2	1.140	1.605	4.76	2	4.20	
4.907	0	1/2	5.36	0.206	4.911	0	2.930	1.565	4.91	0	12.1	0.25
5.070	0	1/2	3.22	0.120	5.059	0	1.630	0.779	5.06	0, 1	6.16	
5.200	0	1/2	1.72	0.061	5.181	0	0.880	0.493	5.17	0, 1	3.90	
5.318	(0)	1/2	0.994	0.034	5.303	···		0.183				
5.413	2	5/2	1.26	0.197	5.389	···		0.264				
5.566	2	5/2	1.33	0.201	5.568	···		0.267				
5.703	2	5/2	6.58	0.98	5.697	12	0.693	0.980	5.71	2	5.11	
5.948	0	1/2	2.15	0.067	5.951	···		0.341(50°)				
6.099	(0)	1/2	1.73	0.052	6.096	···		0.445				
6.27	2	5/2	2.06	0.27	6.262	···		0.190				
6.40	2	5/2	1.15	0.15	6.339	···		0.315				
6.45	2	5/2	2.08	0.27	6.437	···		0.375				
6.81	(2)	5/2	1.06	0.14		···						
6.9	0	1/2	1.53	0.042		···						
7.0	(0)	1/2	3.94	0.106		···						

We believe that the poor resolution relative to the energy level spacings accounts for much of this lack of agreement.

The form of the angular distributions in Fe and an examination of the DWBA calculations suggest that l values can be assigned with a knowledge of the relative intensities at just a few "key" angles, which are approximately 9°, 15°, 25°, and 40°. Accordingly, spectra from the Ni isotopes were measured only at these angles, and l values were assigned with the following standard (derived from the DWBA calculations) as a guide:

$l=0$: $(d\sigma/d\omega)(9°)\approx 3(d\sigma/d\omega)(15°)$, $(d\sigma/d\omega)(15°) > (d\sigma/d\omega)(25°) > (d\sigma/d\omega)(40°)$;

$l=1$: $(d\sigma/d\omega)(9°)\approx(d\sigma/d\omega)(15°)\approx 3(d\sigma/d\omega)(25°)$, $(d\sigma/d\omega)(25°) > (d\sigma/d\omega)(40°)$;

$l=2$: $(d\sigma/d\omega)(9°) < (d\sigma/d\omega)(15°)\approx(25°) \approx 5(d\sigma/d\omega)(40°)$;

$l=3$: $(d\sigma/d\omega)(9°) < (d\sigma/d\omega)(15°)\approx\frac{1}{2}(d\sigma/d\omega)(25°)$, $(d\sigma/d\omega)(25°) > (d\sigma/d\omega)(40°)$;

$l=4$: $(d\sigma/d\omega)(9°) < (d\sigma/d\omega)(15°) < (d\sigma/d\omega)(25°) < (d\sigma/d\omega)(40°)$.

A similar criterion is used for the l assignments to $Ti(d,p)$ reaction proton groups. Figure 5 shows comparisons of experimental points and theoretical curves and illustrates the application of the above method of

TABLE II. $Ni^{58}(d,p)Ni^{59}$.

This paper					MIT reports		Dalton *et al.*			Scott
(1)	(2)	(3)	(4)	(5)	(6)	(7)	(8)	(9)	10)	(11)
Excitation energy (Mev)	l	J	$\left(\frac{d\sigma}{d\omega}\right)_{max}$ (mb/sr)	$(2J_f+1)S$	Excitation energy (Mev)	$\frac{d\sigma}{d\omega}(30°)$ (relative)	Excitation energy (Mev)	l	$(2J_f+1)\theta^2$	$(2J_f+1)S$
0	1	3/2	14.30	2.98	0	1.000	0	1	0.035	1.61
0.340	3	5/2	1.79	4.31	0.341	0.244	0.34	3	0.023	2.64
0.471	1	1/2	7.28	1.41	0.466	0.429	0.47	1	0.019	0.79
0.887	1	1/2	1.88	0.344	0.880	0.152	0.88	1	0.0039	0.20
1.318	1	1/2	3.51	0.600	1.309	0.260	1.32	1	0.0098	
1.696	(3)	(5/2)	0.313	0.580	1.683	0.050				
1.967	4	9/2	0.102	0.383	1.952	0.042				
2.422	1	1/2	0.302	0.043	2.416	0.015				
2.640	3	5/2	0.240	0.358	2.630	0.072				
3.071	4	9/2	2.52	0.790	3.058	0.268	3.05	...	...	
3.203	1	1/2	0.364	0.045	3.193	0.035				
3.421	(0)	(1/2)	1.08	0.060	3.420	0.104	3.45	1	0.0054	
3.468	1	1/2	1.30	0.153	3.457	0.167		and 3	0.19	
3.559	2	5/2	0.871	0.218	3.541	0.181				
3.79	3	5/2	0.062	0.081	3.787	0.015				
3.87	1	1/2	1.12	0.124	3.862	0.137	3.88	...	...	
4.031	1	1/2	0.600	0.065	4.033	0.098				
4.145	1	1/2	0.702	0.078	4.151	0.115				
4.248	1	1/2	1.68	0.178	4.261	0.159(50°)	4.25	...	...	
4.505	2	5/2	7.60	1.64	4.501	1.704	4.50	2	0.047	
4.734	1	1/2	1.42	0.139	4.724	0.145				
4.808	2	5/2	1.42	0.289	4.795	0.268				
4.974	1	1/2	1.40	0.130	4.976	0.091				
5.159	0	1/2	4.13	0.175	5.144	0.723	5.14	0	0.0059	
5.219	2	5/2	0.830	0.035	5.209	0.193				
					5.424	0.109				
5.461	2	5/2	2.61	0.478	5.453	0.425	5.46[a]	2	0.0182	
					5.503	0.161				
5.56	0	1/2	2.34	0.094	5.563	0.295	5.57[a]	0	0.0026	
5.692	0	1/2	4.66	0.183	5.686	0.871	5.69	0	0.0077	0.1
5.890					5.889	1.923	5.90	...	...	
	2	5/2	2.08	0.360	5.918	0.182				
5.940					5.941	0.120				
					5.961	0.125				
6.150	?	?	0.70	...	6.143	0.236				
6.23	2	5/2	0.613	0.100	6.240	0.120				
6.306	2	5/2	1.87	0.302	6.298	0.361	6.28[a]	...	...	
6.380	(0)	1/2	3.72	0.131	6.373	0.858	6.40	...	...	
6.41					6.428	0.057				
	(2)	(5/2)	0.795	0.126	6.447	0.128				
6.49					6.475	0.040				
					6.501	0.157				
6.641	2	5/2	2.39	0.368	6.642	0.567				
					6.702	0.306	6.65[a]	2	0.036	
6.716	2	5/2	3.00	0.448	6.720	0.232				
6.741					6.743	0.391				
					6.912	0.277				
6.96	0	1/2	1.33	0.043	6.948	0.183				
					6.968	0.135				
7.021	0	1/2	1.95	0.059	7.017	0.295				
					7.036	0.134	7.04	...	...	
7.080	(0)	(1/2)	1.53	0.046	7.067	0.389				
					7.086	0.116				
7.199	2	5/2	2.32	0.332	7.198	0.328				
7.448	2	5/2	2.40	0.325	7.449	0.374				
7.595	(2)	(5/2)	2.78	0.371	...	...	7.58	...	...	
7.809	0	1/2	1.20	0.034	...	...				

[a] With other MIT energy [N. B.].

assigning l values. In cases where assignments are available from other work,[9,10] the method used here gives the same result in essentially every case. We have therefore applied this method of assigning l values to levels previously unassigned.

Cross sections used in the above angular distributions have been determined from photographic plate data; the plates have been scanned independently at least twice. Errors in the relative cross sections are estimated to be less than 15%. In obtaining the absolute cross

section, uncertainties in geometrical factors are about 20%.

In the region near $Q=0$, increased background effects and the closeness of the levels causes the results to be somewhat less reliable than results at higher Q values. Below $Q\approx-1$ Mev, the levels cannot be adequately resolved, and DWBA calculations are not available, so that the study was not extended beyond that energy.

The first measurements in this experiment were carried out with 10-Mev deuterons from the Chalk River tandem Van de Graaff accelerator. While these data were not used in the final analysis because measurements were made at only two angles and DWBA calculations are not available for this energy, they were most useful for reaching an understanding of the problems involved and in some cases, for energy calculations.

III. RESULTS

Column (1) of Tables I–IV lists the energy levels found in Ni^{61}, Ni^{59}, Fe, and Ti, respectively. The observed energy levels agree with the MIT data[8,9,12] where they are available, to within about 20 kev; the average deviation is much less. In regions of the spectra where levels are close-lying, the corresponding MIT levels were chosen by comparison of relative cross sections as well as energies. Column (2) of these tables lists the l values we have assigned, and column (3) gives our suggested J values, made on the basis of simple shell model theory (see discussion below). Absolute cross sections at the peaks of the angular distributions are listed in column (4).

Column (5) gives the values $(2J_f+1)S$, obtained from

$$\left(\frac{d\sigma}{d\omega}\right)_{(d,p)}=\frac{(2J_f+1)}{(2J_i+1)}\sigma(\theta,l_n,Q)S(i,f). \qquad (1)$$

The $\sigma(\theta,l_n,Q)$ were obtained from the DWBA calculations.[7] Any uncertainty in this value must be combined with that of the absolute cross sections to determine the uncertainty of S.

We now discuss details of some particular levels:

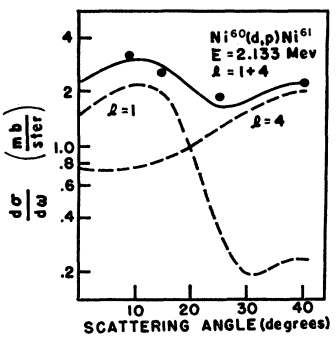

FIG. 6. Fitting of data for 2.133-Mev state of Ni^{61} by combination of DWBA curves for $l=1$ and $l=4$. The individual DWBA curves are shown as dashed lines.

TABLE III. Fe(d,p).

Excitation energy (Mev)	l	This paper J	$\left(\frac{d\sigma}{d\omega}\right)_{max}$ (mb/sr)	$(2J_f+1)S$	MIT Excitation energy (Mev)
0	1	3/2	11.0	2.20	0
0.14	—	—	0.22	···	0.136
0.36	1	3/2	5.52	0.990	0.366
0.71	—	—	0.13	···	0.707
1.26	1	1/2	5.05	0.680	1.266
1.64	1	1/2	0.638	0.082	1.630
1.73	1	1/2	1.56	0.195	1.728
2.14	1	1/2	0.565	0.672	2.124
2.21	3		0.274	0.371	2.212 2.227
2.48	?				2.461 2.511 2.557
2.70	1	1/2	5.56	0.600	2.702
2.920	1	1/2	1.84	0.092	2.928
3.39 3.44	1	1/2	2.11	0.210	3.336 3.375 3.433 3.478
3.98	1 +?	1/2	1.12	0.101	3.943 3.982 4.049
4.16	2 +?	5/2	5.00	0.918	4.139 4.208
4.40	0	1/2	3.42	0.132	4.381 4.412
4.47	2	5/2	1.20	0.211	4.458 4.506
4.58	2	5/2		0.402	4.573 4.594
4.82	0	1/2	6.35	0.220	4.824
4.90	2	5/2	3.97	0.662	4.873 4.902 4.922
5.26	2	5/2	2.06	0.312	5.224 5.241 5.271
5.35	2	5/2	8.40	1.27	5.306 5.364 5.404

Ni^{61}

The experimental points for the peak at $E=2.133$ Mev of Table I have been matched, in Fig. 6, with a combination of theoretical curves for $l=1$ and $l=4$, of almost equal intensities at the peaks. Enge and Fisher[9] have called this simply an $l=1$ transition; Dalton *et al.*[10] have commented that the angular distribution remains high to 60°, a fact consistent with our assignment. Schiffer *et al.*[1] find an $l=4$ level at $E=2.2$ Mev.

In Table I, our data are compared with the results of Enge and Fisher,[9] Dalton *et al.*,[10] and with the DWBA calculations of Scott,[13] which are based on the data of reference 10. In general our spectroscopic factors are about 40% higher than Scott's.

Ni^{59}

The peaks at $E=3.421$ and 3.468 Mev of Table II are not resolvable in the spectra from the isotopic

[13] H. D. Scott, Nuclear Phys. (to be published).

TABLE IV. Ti(d,p).

This paper					Adyasevich *et al.*	Manning *et al.*	Rietjens *et al.*			
(1)	(2)	(3)	(4)	(5)	(6)	(7)	(8)	(9)	(10)	(11)
Q value (Mev)	l	J	$\frac{d\sigma}{d\omega}(10°)$ (mb/sr)	$(2J_f+1)S$	Q value (Mev)	Q value (Mev)	Q value (Mev)	$\frac{d\sigma}{d\Omega}(20°)$ (relative) $Ti^{48}(dp)$	$\frac{d\sigma}{d\Omega}(20)°$ (relative) $Ti^{46}(dp)$	l
							4.16	9±3		···
4.20	···	···	8.48	···	4.14		4.20	43±4		1
3.86	···	···	10.8	···	3.84		3.86		21±4	1
3.76	···	···	0.525	···						
3.55	···	···	0.348	···						
3.48	···	···	0.264	···			3.48	6±3		≥2
3.43	···	···	0.719	···			3.43	7±3		≥2
3.38	···	···	3.29	···			3.38		15±4	1
3.10	···	···	3.96	···	3.09		3.09		18±4	(1)
3.00	1	1/2	1.55	0.174	2.97		2.98		40±6	(1)
2.75	1	1/2	6.16	0.670			2.75	27±6		(1)
							2.73		83±10	(1)
2.66	1	1/2	9.52	1.02			2.66	55±2		(1, 2)
2.48	1	1/2	0.880	0.0930	2.53	2.457				
2.27	1	1/2	0.352	0.0363	2.27					
2.13	1	1/2	3.38	0.335		2.184				
2.00	1	1/2	0.514	0.0504		2.001				
1.83	0	1/2	0.938	0.0413						
1.78	1	1/2	0.733	0.0685						
1.68	1	1/2	1.84	0.169						
	3	5/2	0.675	0.710						
1.54	0	1/2	0.930	0.0390						
	3	5/2	0.220	0.232						
1.49	1	1/2	2.90	0.261						
1.40	1	1/2	2.73	0.264						
	3	5/2	0.915	0.955						
1.32	1	1/2	0.952	0.0828						
1.24	1	1/2	2.41	0.226	1.24	1.211				
1.14	4	9/2	1.52	3.66						
	1	1/2	1.47	0.123						
1.00	1	1/2	5.20	0.433	1.04	1.041				
	3	5/2	1.17	1.31						
0.91	0	1/2	1.69	0.0637	0.96	0.960				
0.79	1	1/2	9.90	0.805						
0.73	3	5/2	1.36	1.30						
0.66	0	1/2	0.740	0.0270						
0.57	1	1/2	0.542	0.0420						
	3	5/2	0.205	0.190						
0.49	0	1/2	2.83	0.101						
0.21	1	1/2	1.30	0.0964						
0.17	1	1/2	1.41	0.103						

target but can be resolved in the spectra from the natural nickel target. From the latter spectra, the ratios of the two peak heights were taken, and the cross section observed on the isotropic spectra (where the cross sections are more reliable) was divided between the two peaks according to this ratio. The two resulting distributions are shown in Fig. 7. On the basis of 9° and 15° data, the peak at 3.421 Mev may be assigned to an $l=0$ transition; the other peak has $l=1$.

The last column of Table II lists Scott's[13] values of $(2J_f+1)\theta^2$, which should be directly comparable to our values in column (5). It may be noted that the $(2J_f+1)S$ values are again higher than the corresponding values of Scott (who also used DWBA methods) by about 40%.

Iron

In the iron spectra some proton groups have not been resolved, and some other broad peaks are due to the combined effect of two or more close-lying levels. We have been able to distinguish only one proton group corresponding to an $l=3$ transition. For some of the combined levels, however, it is possible to fit the experimental points, which are relatively high in the 25°–40° range, by superposing theoretical curves for $l=1$ plus $l=3$ or 4. (See Fig. 8.) Other broad peaks can be fitted by $l=2$ plus $l=3$ or 4 curves. From these considerations we infer the presence of levels corresponding to $l>2$ transitions, but we cannot determine their energies or corresponding cross sections accurately.

Ti

Since the abundance of Ti^{49} is 74% whereas no other single isotope has an abundance greater than 8% in natural titanium, the cross section of each level is calculated on the assumption that the level is one of Ti^{49} unless it coincides with a known level of Ti^{47}. Since the region near the ground state has been studied

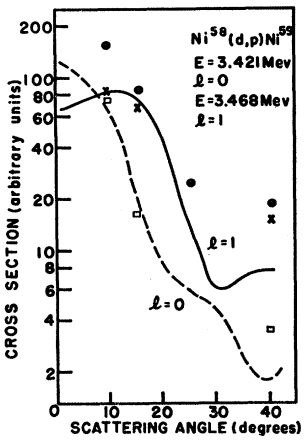

FIG. 7. Analysis of angular distribution for 3.4-Mev states of Ni^{59}. Dots are measured points, crosses and squares are portions of total count assigned to the 3.468-Mev level and 3.421-Mev level, respectively, on the basis of higher resolution data. The dashed and solid lines are DWBA curves for $l=0$ and $l=1$, respectively. See discussion in text.

previously,[14,15] the principal concentration in this work is in the region below $Q=3$ Mev.

Our $Q=3.00$-Mev peak probably contains the 2.97-Mev Ti^{49} peak of Adyasevich *et al.*[15] and the 2.98-Mev peak of Ti^{47} found by Rietjens, Bilaniuk, and Macfarlane.[14] Our 3.10-Mev level coincides with one found in Ti^{49} in reference 15, and with a level found in Ti^{47} in reference 14.

Five $l=3$ values and one $l=4$ value were assigned after matching the experimental curve for a particular peak with an $l=1$ experimental curve from a neighboring peak and an $l=3$ (or 4) curve from the DWBA calculations. In these cases, the cross section for each part of the double peak was taken according to the ratio of the individual superposed curve to the total cross section. A typical example is shown in Fig. 9.

Note that only one proton group corresponding to an $l=4$ transition was detected. That such detection is difficult is indicated from the DWBA calculations for $l=4$, $Q=0$: the angular distribution up to 40° shows few distinguishing features. For higher Q values, the curve shows a more pronounced rise at 40°, thus making detection of such peaks easier, but we found no $l=4$ peaks even in this region. For no peak in the analyzed spectra was the intensity at 40° greater than that at 25°.

It is also noteworthy that we found no $l=2$ peaks in the spectra. The angular distribution for $l=2$ is quite characteristic above $Q\simeq 0$ and should be easily detectable.

IV. ANALYSIS AND DISCUSSION

The principal experimental effort, and the clearest interpretations in this work are in the nickel isotope data. The Fe and Ti data are less reliable experimentally because of the poorer energy resolution coupled with higher level densities and the presence of many isotopes,

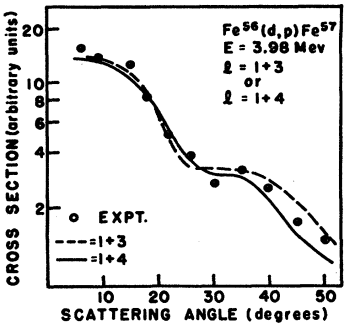

FIG. 8. Analysis of angular distribution for 3.98-Mev state in Fe^{57}. See discussion in text.

and the theoretical interpretations are clouded by couplings between the neutrons and protons (for example, the problem of non-single-closed-shell nuclei has not been successfully treated by pairing theory). In this section, we therefore concentrate our interest on the nickel isotope data, although much of the discussion also applies to the Fe and Ti data.

Perhaps the most interesting application of the results is to determine the location of the single-particle (i.e., shell model) states, E_j. We take these as the "centers of gravity" of the reduced widths, or

$$E_j=\sum_i S_iE_i/\sum_i S_i, \tag{2}$$

where the summation is over all nuclear states belonging to a given shell model state, j. The values of $\sum S$ and E_j obtained from Tables I–IV are presented in columns (2) and (3) of Table V. Columns (4) and (5) of Table V gives the predictions of pairing theory[16] for $\sum S$ and E_j.

It has been shown[17,18] that

$$\sum_i S_i=U_j^2,$$

where U_j^2 is a quantity defined and calculated along with E_j for the nickel isotopes in reference 16. For states well above the ground state, any theory would predict $\sum S=1.0$.

In deriving Table V from Tables I–IV, there is of course an uncertainty in assigning an $l=1$ state as $p_{3/2}$ or $p_{1/2}$ except for the ground states which are known

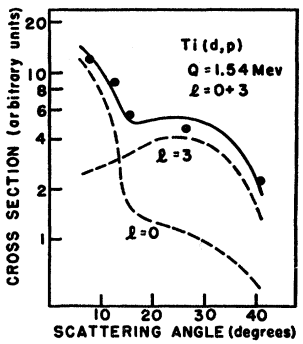

FIG. 9. Analysis of angular distribution for 1.54-Mev state excited in Ti(d,p). Dashed curves are DWBA calculated angular distributions for $l=0$ and $l=3$, and solid curve shows how a combination of these is fit to the data.

[14] L. H. Th. Rietjiens, A. M. Bilaniuk, and M. H. Macfarlane, Phys. Rev. **120**, 527 (1960).
[15] B. P. Adyasevich, L. V. Groshev, and A. M. Demidov, J. Nuclear Energy **3**, 258 (1956) and Soviet. J. of Atomic Energy **2**, 40 (1956).
[16] L. S. Kisslinger and R. A. Sorenson, Kgl. Danske Videnskab. Selskab, Mat.-fys. Medd. **32**, No. 9 (1960).
[17] S. Yoshida, Phys. Rev. **123**, 2122 (1961).
[18] B. L. Cohen and R. E. Price, Phys. Rev. **121**, 1441 (1961).

to be $p_{3/2}$. The best agreement with pairing theory predictions of $\sum S$ is obtained if all other states are assigned as $p_{1/2}$. In Ni^{61}, this agreement is exceedingly good, and it would become exceedingly bad if, for example, the first excited $l=1$ state were assigned as $p_{3/2}$ instead of $p_{1/2}$. In Ni^{59}, the absolute agreement is not overly good in either case, but the ratios of $\sum S$ for $p_{3/2}$ and $p_{1/2}$ is much closer to theoretical predictions if the first excited $l=1$ state (0.471 Mev) is assumed to be $p_{1/2}$. As a further check, a measurement was made of the ratio of the cross sections for exciting the ground and 0.471-Mev states by (d,t) reactions.[19] If the 0.471-Mev state were $p_{3/2}$, the ratio should be the same as in (d,p) reactions, about 2.0; if it were $p_{1/2}$, the ratio should be very much larger than this. The observed ratio was 8.0, which supports the $p_{1/2}$ assignment (a discussion of some of the limitations of this method is given in reference 20).

In obtaining Table V from Tables I–IV, there is also an ambiguity in the assignment of $l=2$ states as $d_{5/2}$ or $d_{3/2}$. There was no apparent energy gap in the $l=2$ levels observed, and $\sum S$ for all of these was slightly less than the expected value of unity if all are assigned as $d_{5/2}$. From shell model, one expects the $d_{3/2}$ to be several Mev above the $d_{5/2}$, so that all observed levels were taken to be $d_{5/2}$.

In general, there is quite reasonable agreement between the experimental and theoretical values of $\sum S$; the principal discrepancy is in the case of the $s_{1/2}$ levels, where the observed value is less than half of the theoretical. Since $s_{1/2}$ levels occur with undiminished frequency up to the highest energy studied, the small experimental values of $\sum S$ may be interpreted as an indication that only about half of the $s_{1/2}$ levels have been observed, and that the rest lie above the energy region studied. The actual E_j is therefore near the highest energy studied in this experiment rather than at the energy listed in Table V.

The locations of the single particle levels taken from Table V (except for the $s_{1/2}$ case discussed above) are shown in Fig. 10, where they are compared with the results of reference 1. One immediately notes that the discrepancies between this work and reference 1 are very large. Moreover, the most important discrepancies between reference 1 and the theoretical expectations discussed in the Introduction have been removed. There is now a large energy gap between the major shells, and even reasonably large gaps between $p_{1/2}$ and $g_{9/2}$ and between $d_{5/2}$ and $s_{1/2}$, in agreement with the facts that 40 neutrons or protons and 56 neutrons have some of the properties of closed shells.[20] The $3s_{1/2}$ state is now near zero binding energy as expected from our knowledge of the neutron giant resonance, and from its energy shift between masses 60 and 90–120. The binding energies of the highly-excited states vary smoothly with A within the limitations of the available evidence. For states near the ground state, relatively rapid variations with A are expected theoretically.

Another demonstration of the comparison between the present data and those of reference 1 is shown in Fig. 11. Here the various nuclear levels belonging to each shell-model state in the nickel isotopes are shown by lines of height proportioned to their reduced widths. The "centers of gravity" determined from this work are

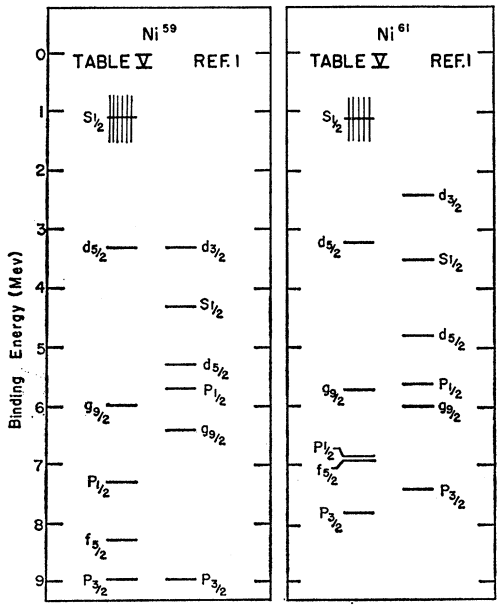

FIG. 10. Location of single-particle levels in Ni^{59} and Ni^{61}. Results designated "Table V" are from this work; the locations of $s_{1/2}$ level are somewhat uncertain. See discussion in text.

[19] The authors are indebted to J. E. Hay for making this measurement.

TABLE V. Results for Ni^{58} and Ni^{60} and comparison of with predictions of pairing theory.

(1) State	Experimental (2) ΣS	(3) E_j (Mev)	Pairing theory[a] (4) ΣS	(5) E_j (Mev)
	(a) $Ni^{60}(d,p)Ni^{61}$			
$p_{3/2}$	0.40	0	0.43	0
$f_{5/2}$	0.84	0.9	0.76	0.01
$p_{1/2}$	0.98	0.9	0.90	0.43
$g_{9/2}$	0.62	2.1	0.99	>3.11
$d_{5/2}$	0.95	4.6	1.0	>4
$s_{1/2}$	0.47	4.6[b]	1.0	>4
	(b) $Ni^{58}(d,p)Ni^{59}$			
$p_{3/2}$	0.75	0	0.68	0
$f_{5/2}$	0.89	0.7	0.90	0.34
$p_{1/2}$	1.6	1.7	0.96	0.96
$g_{9/2}$	0.83	3.0	0.99	>3.76
$d_{5/2}$	0.90	5.7	1.0	>4
$s_{1/2}$	0.41	5.8[b]	1.0	>4

[a] See reference 16.
[b] This is center of gravity of observed levels. As discussed in text, taking account of $s_{1/2}$ levels in region not investigated increases E_j for $s_{1/2}$ by about 2 Mev.

[20] B. L. Cohen, Phys. Rev. **125**, 1358 (1962).

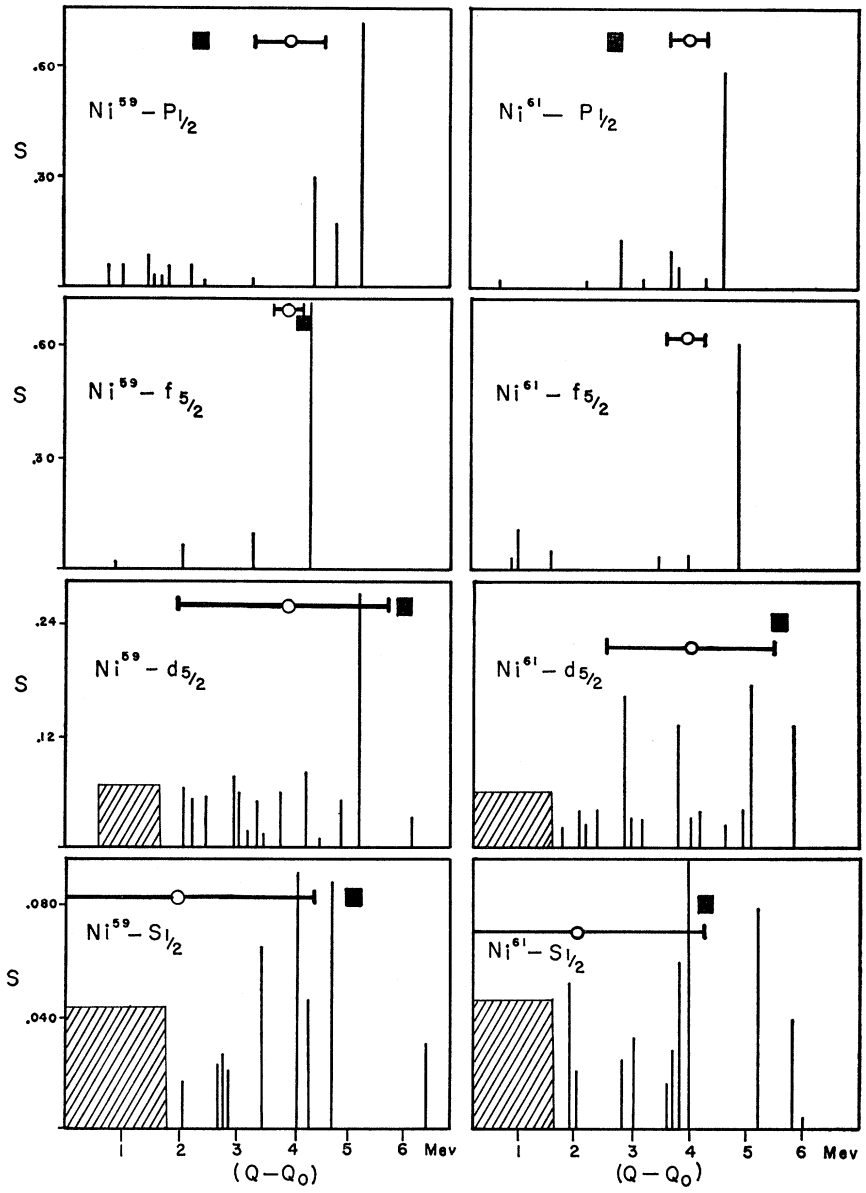

FIG. 11. Nuclear levels found in this work belonging to the shell model states designated. Vertical lines represent positions of levels, and their heights show the S values from Tables I and II; the latter are roughly proportional to the cross sections. The cross-hatched areas designate regions not investigated in these experiments. The open circles designate the center of gravity of these levels reported in Table V (see text for discussion of $s_{1/2}$ case). The horizontal bars centered on the open circles designate the width of the single-particle levels expected from giant resonance theory. The black squares show the locations of the single-particle levels reported in reference 1. The quantity Q_0, the origin of the abscissa scales, is different for each diagram; its value can be obtained from the equation $Q_0=Q_{gs}-E_j-4$ Mev, where Q_{gs} is the ground-state Q value and E_j is found in column (3) of Table V.

shown by the open circles, and the energies given in reference 1 are denoted by the black squares.

Figure 11 also gives an indication of the energy distribution of the levels belonging to a single shell-model state. In accordance with the theory of Lane, Thomas, and Wigner,[2] the width of this distribution should be approximately equal to the depth of the imaginary potential, W, used in optical model calculations. For 0–4-Mev neutron induced reactions, in which the compound nucleus excitation energy E^* averages about 10 Mev, optical model fits[21] require $W\approx 3$ Mev. Optical model fits to proton elastic scattering data[21] use $W\approx 7$ Mev at $E^*=18$ Mev, $W\approx 8.5$ Mev at $E^*=25$ Mev, and $W\approx 15$ Mev at $E^*\approx 45$ Mev. All of this is roughly consistent with

$$W\approx 0.33E^*. \tag{3}$$

It is theoretically plausible[22] that the validity of (3) should extend down into the region investigated in this paper, where E^* is just the excitation energy E_j. The values of W predicted by (3) are shown in Fig. 11 as horizontal bars centered on E_j.

In comparing the size of these bars with the widths of the distribution in energy of the observed levels, one observes that the agreement is quite good. This serves to support our assumptions that all of the $l=2$ states

[21] H. Feshbach, in *Nuclear Spectroscopy*, edited by F. Ajzenberg-Selove (Academic Press, Inc., New York, 1960), Part A–B.

[22] This was pointed out to the authors by G. E. Brown.

TABLE VI. Summary of results for iron and titanium.

State	ΣS	E_j (Mev) Table III	E_j (Mev) reference 1
	(a) Iron		
$p_{3/2}$	0.80	0	0.3
$f_{5/2}$	0.06	2.1	···
$p_{1/2}$	1.30	2.1	2.2
$g_{9/2}$	···	···	(3.2)
$d_{5/2}$	0.63	4.7	2.3
$s_{1/2}$	0.18	4.6	4.7
	(b) Titanium		
$f_{5/2}$	0.78	4.8	2.5
$p_{1/2}$	2.5	4.1	3.1
$g_{9/2}$	0.37	4.8	3.8
$d_{5/2}$	···	···	4.3
$s_{1/2}$	0.14	4.9	4.9

are $d_{5/2}$, and that about half of the $s_{1/2}$ states are in the region above that studied in these experiments. It should perhaps be pointed out that the bars in Fig. 11 are twice as wide as those in an earlier unpublished vresion of this paper; this error arose from the fact that the W used in reference 2 is twice as large as the W commonly used as the depth of the imaginary potential well.[22]

Another interesting aspect of the results reported here is the comparison of the observed values of $\sum S$ and E_j for the $p_{3/2}$, $p_{1/2}$, and $f_{5/2}$ states with the predictions of pairing theory.[16] This is shown in Table V, where it is seen that the agreement is very good; in fact it is probably much better than one should expect in view of the many uncertain parameters in the pairing theory calculations, the approximations in the DWBA computation, and the uncertainty in the measured absolute cross sections. It should be kept in mind, however, that there was some arbitrariness in the division of the $l=1$ states between $p_{3/2}$ and $p_{1/2}$.

A summary of the results for iron and titanium is given in Table VI. It is clear from the $\sum S$ values that many levels are missed, or their l values are improperly assigned. This is at least partly due to the inadequate energy resolution relative to the level spacing and to the uncertain isotopic assignments. In Ti, there was the additional complication that the data were analyzed using the DWBA calculation for Fe. In spite of the uncertainties, there are still some important discrepancies with the results of reference 1. Since $s_{1/2}$ states could not be easily missed, the small values of $\sum S$ for the $s_{1/2}$ states indicate that the major contribution to this shell-model state are in the high-energy region not investigated in this experiment.

ACKNOWLEDGMENTS

A very special debt of gratitude is due E. Almqvist and J. A. Kuehner for arranging and supervising the runs on the Chalk River tandem Van de Graaff with which this project was initiated. The authors are also greatly indebted to G. R. Satchler for providing the DWBA calculations, and to N. Austern, G. E. Brown, and E. Rost for very helpful theoretical discussions.